

# Anomalous Hall Effect in Bismuth

Bruno Cury Camargo,\* Piotr Gierłowski, Maciej Sawicki, and Katarzyna Gas

*Institute of Physics, Polish Academy of Sciences,  
Aleja Lotników 32/46, PL-02-668 Warsaw, Poland.*

Andrei Alaferdov and Yakov Kopelevich

*Instituto de Física Gleb Wataghin, R. Sergio Buarque de Holanda 777, 13083-859 Campinas, Brazil.*

Iraida N. Demchenko

*University of Warsaw, Department of Chemistry, ul. Pasteura 1, PL-02-093 Warsaw, Poland.*

(Dated: February 4, 2020)

We report the occurrence of ferromagnetic-like anomalous Hall effect (AHE) below 30 mT in bismuth single and polycrystals. The signatures of ferromagnetism in transport are not corroborated in magnetization measurements, thus suggesting the induction of non-intrinsic magnetism at surfaces and grain boundaries in bismuth. The suppression of the AHE with the increase of magnetic field and temperature coincides with previous reports of superconductivity in Bi, suggesting an interplay between the two phenomena.

## I. INTRODUCTION

Bismuth (Bi) is perhaps the original wonder material. Historically, it has been the catalyst for the discovery of different phenomena that make today the bedrock of condensed matter physics such as the Shubnikov-de Haas, de Haas-van Alphen, Seebeck and Nernst effects<sup>1–3</sup>. In addition to those, more recently, Bi has been shown to host intrinsic superconductivity, and to behave as a higher order topological insulator - a testament to its unusual properties<sup>4,5</sup>.

Being a material with low charge carrier concentration ( $\approx 10^{17} \text{ cm}^{-3}$ ), low carrier effective masses ( $\approx 10^{-3} \text{ m}_e$ ) and a small density of states at the Fermi level ( $N(0) \approx 0.1 \text{ eV}^{-1}$ )<sup>6–10</sup>, Bi is susceptible to Fermi surface reconstructions, which manifest as exotic electronic states. These can be triggered by defects or external parameters, such as magnetic field and pressure<sup>11–13</sup>. It is known, for example, that Bi undergoes a metal-to-insulator transition when exposed to magnetic fields of the order of few Tesla. At present, such behavior has different interpretations, including the coexistence of electrons and holes within the two-band model<sup>14</sup>, the development of an excitonic gap and the occurrence of magnetic-field-induced electron-electron pairing<sup>11</sup>.

Historically, the magnetotransport properties of bismuth have been studied at high magnetic fields (above 1 T), partially due to intriguing properties such as linear magnetoresistance, strong spin-orbit coupling and the relatively low magnetic fields necessary to attain the quantum limit<sup>15,16</sup>. Here, we focus on the low magnetic field magnetoresistance. We demonstrate the occurrence of hysteresis loops in Hall measurements consistent with the presence of magnetic ordering in Bi which, being one of the most diamagnetic non-superconducting materials known to men, is not expected to exhibit either ferro- or antiferromagnetism.

## II. SAMPLES AND EXPERIMENTAL DETAILS

We investigate samples cut from Bi crystals grown by the Bridgman method, with 5N purity (see the sample characterization in the Supplementary information). The specimens had dimensions of approx.  $5 \text{ mm} \times 3 \text{ mm}$  (in-plane) and thickness varying between 0.5 mm and 1 mm. Experiments comprised of electrical resistivity and magnetization measurements. Measurements were carried out in the temperature range  $2 \text{ K} \leq T \leq 10 \text{ K}$ , with magnetic fields  $-30 \text{ mT} \leq \mu_0 H \leq 30 \text{ mT}$ .

Longitudinal and transversal resistivity measurements were performed in a homemade  $\text{He}_4$  cryostat and a Quantum Design 9T PPMS instrument. Samples were contacted in the standard five-probe geometry using gold wires, which were either directly soldered to the sample surface or glued in place with non-superconducting silver epoxi. Measurements were performed both with DC and AC excitation currents with various amplitudes. Experiments in the presence of magnetic fields were performed in the zero-field-cooled (ZFC) and field-cooled (FC) regimes. Between measurements, the sample was systematically subjected to demagnetization at  $T = 10 \text{ K}$ , from a field of 1 T. Such procedure aimed at achieving consistent remnant fields in the superconducting coil.

Magnetization measurements were carried out in a MPMS XL Superconducting Quantum Interference Device (SQUID) magnetometer equipped with a low field option. A special degaussing procedure has been applied and a soft quench of the superconducting magnet executed prior the measurements to assure a below 0.1 mT magnitude of the trapped field the sample chamber during our weak field measurements. Customary prepared long Si strip facilitated the samples support in the magnetometer chamber and we strictly followed the experimental code and data reduction detailed in Ref. 17.

### III. RESULTS AND DISCUSSION

The main result of the present report is shown in Fig. 1. Measurements in all our devices revealed featureless  $R(T)$  curves in the absence of magnetic fields. For small values of  $\mu_0 H$ , however, a sharp resistance reduction (accounting for up to 25% of the sample resistance) was observed below 4 K. The transition was suppressed by magnetic fields, surviving up to  $\mu_0 H \approx 20$  mT.

The presence of such transition was strongly dependent on the samples magnetothermal history. It was triggered below a certain temperature  $T^*$ , associated to an irreversible behavior in the  $R(T)$  curves (see Fig. 1). Resistance drops were observable only in ZFC measurements, whereas curves obtained during FC runs did not demonstrate any features below 5 K.

$R(T)$  measurements performed with different temperature sweeping rates and at thermal equilibrium yielded identical results. Similarly, no frequency-dependency was observed on AC resistivity for frequencies up to 1 kHz.  $I-V$  characterizations in the ZFC and FC branches of the  $R(T)$  curves revealed ohmic behavior, and no relaxation was observed at  $T = 2$  K in measurements spanning eight hours. These results weigh against a charge density wave as the source of the hysteresis observed. They do not discard, however, the possibility of a glassy state with typical relaxation times above several hours.

Instead, the presence of irreversibility in our  $R(T)$  measurements can be attributed to the existence of small, randomly-aligned regions with single magnetic domains within the material, as large regions would be more likely to host domain walls and therefore produce loops with

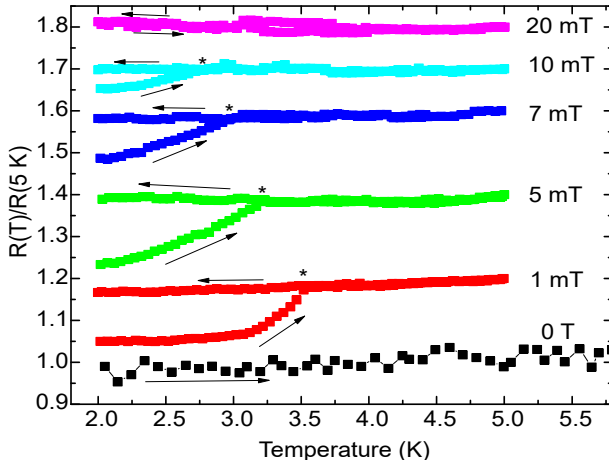


FIG. 1. Normalized  $R(T)$  measurements for the Bi sample. The curves have been displaced vertically for clarity. The direction of the measurements are indicated by arrows. Measurements at zero field and at 20 mT presented reversible behavior. The other curves presented an irreversibility between the heating and cooling cycles, indicated by stars. ZFC curves yielded a sharp resistance increase above a certain temperature.

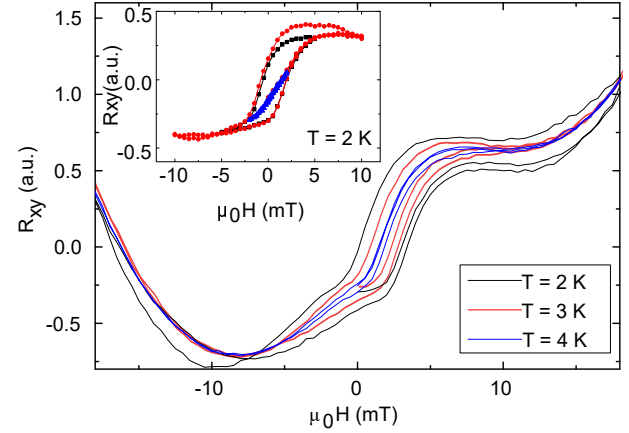


FIG. 2. Hall component of  $R_{xy}$  measurements at  $T = 2$  K, 3 K and 4 K (See the supplementary material for information on how the curves were obtained). A behavior resembling a ferromagnetic hysteresis developed below 4 K. The inset shows  $R(H)$  loops at  $T = 2$  K, with maximum magnetic fields  $\mu_0 H = 2$  mT, 5 mT and 10 mT.

larger ZFC resistances than those in the FC regime. In the ZFC condition, the pinning of domains at small applied  $\mu_0 H$  ensures a sample with weaker macroscopic magnetic response than at higher temperatures. In the FC regime, however, the cooling in the presence of  $\mu_0 H \neq 0$  ensures the same effective field above and below  $T^*$ , suppressing the transition.

Such hypothesis is corroborated by magnetoresistance measurements below  $T^*$ , which revealed a hysteretic behavior compatible with the presence of pinned magnetic domains. The hysteresis observed in the antisymmetric component of  $R_{xy}$ , shown in Fig. 2, resembled the ones found in the anomalous Hall component of ferromagnets. The temperature dependence of the coercive field in such loops presented an activated behavior, of the type

$$\mu_0 H = 0.96 \times \frac{K_1}{M_S} \left[ 1 - \left( \frac{T}{T_0} \right)^{\frac{3}{4}} \right], \quad (1)$$

with  $K_1/M_S \approx 3.6 \times 10^{-3}$  T the ratio between the anisotropy density of the magnetic centers  $K_1$ , and their magnetization  $M_S$ . For our samples,  $T_0 \approx 4.0$  K, which is close to the critical temperature obtained by mapping the irreversible behavior of the  $R(T)$  curves at different magnetic fields ( $T_0 \approx 3.9$  K). A diagram with the results is presented in Fig. 3.

The relation expressed in Eq. 1 corresponds to the coercivity of a non-interacting assembly of single domain magnetic particles with blocking temperature  $T_0$ <sup>19</sup>. The exponent 3/4 corresponds to the case when their easy axis is randomly-oriented in relation to the magnetic field<sup>20</sup>. Such observation in Hall measurements suggests that our samples present weak, diluted magnetism. Magnetization measurements, however, yielded no signs of

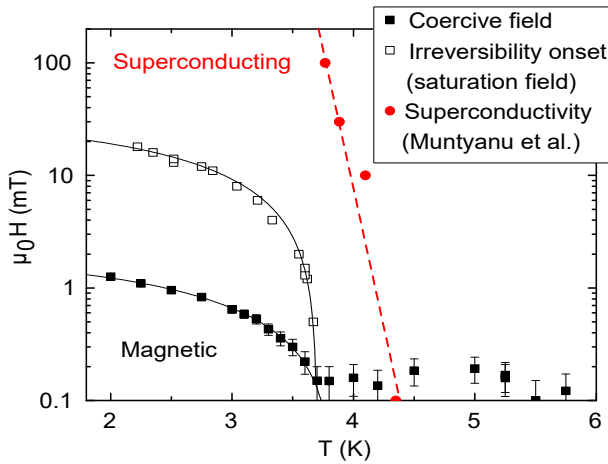


FIG. 3. Magnetic field vs. temperature diagrams for the coercive field (black closed squares) and irreversibility temperature (open squares) of the magnetic phase of Bi, and magnetic field as a function of temperature (red circles) for the superconducting phase of bismuth. The data for the latter was extracted from Ref. 18. The dashed line is a guide to the eye. The full lines were obtained from Eq. 1 with  $T_0 = 4.0$  K and  $K_1/M_s = 3.6$  mT for the closed squares and  $T_0 = 3.9$  K and  $K_1/M_s = 50$  mT for the open squares.

ferromagnetic-like behavior within experimental resolution, as shown in Fig. 4. The  $M(T)$  dependency was diamagnetic and only at the lowest  $T$  a weak Curie-Weiss paramagnetic signal emerged, Fig. 4 a). Neither the nonlinear component of the diamagnetic-dominated  $M(H)$  data (see the Suppl. Material, Fig. S6), shown in Fig. 4 b), points to ferromagnetic-like behavior. Rather, all features present in it can be attributed to weak irreducibilities of the magnet power supply, as pointed out in 21. Combined, these observations further indicate a very small volumetric fraction as the responsible for the phenomenon found in electrical transport measurements.

Indeed, elemental analysis of the samples did not reveal the presence of magnetic impurities (see the Suppl. Material). Combined to magnetization measurements, such results attest against magnetic contaminants as the source of the AHE. For example, taking the saturation magnetization of iron<sup>22</sup> at  $M_{sat} \approx 2.73 \times 10^{-4}$  Am<sup>2</sup>/kg, the absence of signatures of magnetism down to  $10^{-10}$  Am<sup>2</sup> ( $910^{-7}$  Am<sup>2</sup>/kg) puts an upper limit for Fe impurities at 5  $\mu$ g in our 0.111 g sample, accounting for an amount below 45 parts per million in mass. For magnetite (Fe<sub>2</sub>O<sub>3</sub>,  $M_{sat} \approx 9.42 \times 10^{-5}$  Am<sup>2</sup>/kg), a similar estimation places an upper limit of approx. 120 ppm in mass<sup>23</sup>.

Considering the larger value estimated above, and supposing that magnetism in our sample has magnetite as origin, the observed magnetic signal would originate from, at most, 200 ppm of the total sample volume (ca.  $2.3 \times 10^{-12}$  m<sup>3</sup>, whereas the entire sample has approx.  $10^{-8}$  m<sup>3</sup>). Taking the noise level of the  $M(H)$  measure-

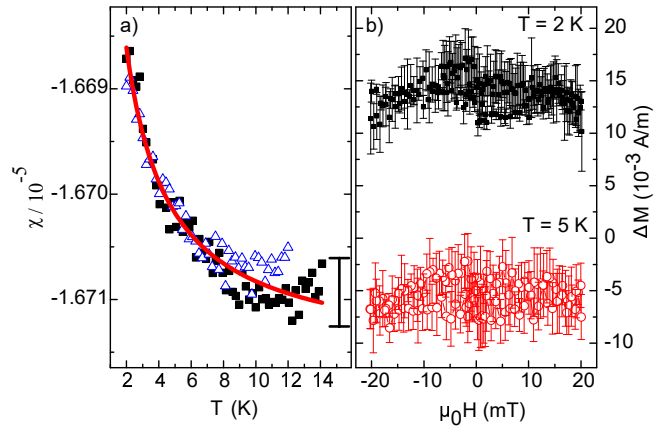


FIG. 4. a) ZFC (full black squares) and FC (blue open triangles)  $\chi(T)$  curves at  $\mu_0 H = 10$  mT, showing a weak Curie-like paramagnetic contribution  $M \approx M_0 + C \times H/T$ , with  $C \approx 7.2 \times 10^{-3}$  K (red line). The bar on the bottom right corresponds to the experimental uncertainty. b) Nonlinear part of the magnetization hysteresis loops obtained by the subtraction of a linear diamagnetic background  $\Delta M(H) = M(H) - \alpha H$ . Measurements were performed at  $T = 2$  K (closed black symbols) and  $T = 5$  K (open red symbols). Curves are shifted vertically for clarity.

ments ( $\approx 10^{-10}$  Am<sup>2</sup>) as the upper limit for the saturation magnetic moment of magnetite nano-precipitates amounts for an estimated volume magnetization of the magnetic centers  $M_S \approx 44$  A/m. From the experimental ratio  $K_1/M_S \approx 3.6$  mT (see Eq. 1), we obtain  $K_1 \approx 0.154$  J/m<sup>3</sup>. This value is unreasonably small (typical values for  $K_1$  range between  $10^4$  and  $10^5$  J/m<sup>3</sup>, and can average only to no less than  $10^2$  J/m<sup>3</sup> in soft nanocrystalline magnets<sup>19,24</sup>), allowing for a re-estimation of the magnetic volumetric fraction of the sample at least three orders of magnitude below 200 ppm (which would increase  $M_S$ , and therefore,  $K_1$  accordingly). This new number is consistent with impurity quantities estimated from the weak paramagnetic background in  $M(T)$  measurements, which yields an estimated concentration of PM =  $1.4 \times 10^{15}$  S = 2 spins per gram in the sample. Assuming one spin per foreign atom and taking into account the molar mass of Bi at 83 g/mol, this results in a total atomic impurity amount of the order 0.2 ppm.

Such small fractions cannot be held accountable for the  $\approx 20\%$  variation observed in  $R(T)$ , as well as the clear hysteresis loops found in Hall measurements. We also note that the transition temperatures found in the experiments, to the best of our knowledge, do not coincide with the typical Curie temperatures of such magnetic contaminants. One way to reconcile our findings in  $M(T)$  and  $R(T)$ , is to consider the AHE originating at the surface or grain boundaries of Bi, rather than caused by diluted contaminants.

Surely, it has been demonstrated that surface conductivity in bismuth plays a large role in the macroscopic

sample resistivity<sup>25</sup>. In particular, it was shown that surface adsorption of gas, dislocations and rotations between crystalline regions can cause the reconstruction of the materials Fermi surface, inducing unusual metallicity and exotic electronic states such as superconductivity<sup>18,26,27</sup>. In addition, a recent report revealed that hinge states in Bi along the binary direction house topological states<sup>5</sup>. Such manifestation of the spin-Hall effect in the absence of detectable signs of magnetism, could in principle be held accountable for triggering the AHE observed here.

However, measurements performed before and after an in-situ heat treatment in vacuum ( $10^{-3}$  Torr at  $T = 370$  K for 4h) yielded no observable changes. This points against a purely surface-related phenomenon, as doping caused by adsorbed gases would require a variation of the magnetic properties with the coating, as seen for example - in graphite<sup>28</sup>. This result indicates grain boundaries as the most likely candidate to exhibit magnetism in the system.

When considering grain boundaries, the development of a FM-like AHE below 4 K becomes a puzzling factor. While the absence of the Meissner effect and the lack of transitions in FC  $R(T)$  measurements attest against the occurrence of superconductivity, a transition temperature  $T^* = 3.9$  K is indeed close to previous reports of superconductivity in the system (around 4.1 K)<sup>27,29</sup>. This is illustrated in Fig. 3. We note, however, that superconductivity in Bi is usually more complex than the phenomenon reported here, with multiple subsequent transitions expected around 4.1 K and 8.4 K. Meanwhile, in our samples, no anomaly was observed above 4.1 K. In addition, the magnetic fields necessary to completely saturate the hysteresis loops in our devices were one order of magnitude below the critical fields reported for superconductivity in bismuth bicrystals<sup>29</sup> (see Fig. 3). These observations, combined, weigh against superconductivity as the source of the magnetism (i.e., the AHE) in our samples. It is possible, however, that both phenomena might be related, with magnetism playing as a precursor of superconductivity, which can be tuned by disorder.

The superconductivity reported in bismuth is expected to happen either on its amorphous phase or on interfaces regions within the sample<sup>27,29,30</sup>. As such, this phenomenon is not intrinsic of Bi, but rather a consequence of the reconstructed Fermi surface along grain boundaries. In particular, it has been experimentally demonstrated<sup>18</sup> that such faults present a three orders of magnitude larger density of states in comparison with crystalline Bi, thus suggesting a reconstruction involving wide band dispersion along dislocations.

Assuming the Curie temperature of the magnetic transition at  $T_C \approx 4$  K (i.e. where the coercive field vanishes), and magnetism in our sample as having itinerant origin, we estimate the Stoner exchange parameter  $I$  that would give origin to the magnetism<sup>31</sup>

$$I \approx \frac{1}{N(0) \left( 1 - \alpha \left( \frac{k_B T_C}{E_F} \right)^2 \right)} \approx 10 \text{ eV}, \quad (2)$$

with  $E_F \approx 0.27$  meV the Fermi energy<sup>6</sup>,  $N(0) \approx 0.1 \text{ eV}^{-1}$  the density of states or Bi at the Fermi level<sup>10</sup> and  $\alpha$  a constant below one<sup>10,31</sup>. Such a value is around three orders of magnitude above those typical for known ferromagnetic materials, such as Fe ( $I_{\text{Fe}} \approx 0.6$  eV)<sup>32</sup>. Such an overestimation can be attributed to an inappropriate value of  $N(0)$ , which is unrealistic in the regions likely responsible for magnetism in our samples as discussed above. Taking a three orders of magnitude higher density of states at the Fermi level along grain boundaries into account<sup>18</sup>, we obtain a Stoner exchange parameter of the order of  $I \approx 10$  meV.

The wide band dispersion responsible for the inflated density of states can be understood in view of the natural strain and stresses present in the system. Such features are expected to create an effective potential vector in the material, which under certain conditions can be held accountable for flat band states<sup>33</sup>. In our samples, in which crystal grains are grown at random, the presence of strains satisfying the conditions necessary for the induction of the flat-band states would be satisfied only in a fraction of all the grain boundaries. Suitably, the magnetic volumetric fraction previously estimated with basis on  $M(T, H)$  measurements revolves around few ppm.

Flat bands have recently been focus of intense experimental work in twisted multilayer graphenes, in which instabilities towards ferromagnetic and superconducting order are triggered depending on the sample doping (see e.g. 34 and references therein). Similarly, we argue that a reconstruction of the Fermi surface of Bi towards a flat dispersion at crystalline edges can be held accountable for the exotic phenomena observed, with the presence of larger density of states and superconductivity along such regions having already been previously reported<sup>29</sup>. The triggering of ferromagnetism, however, has not yet been observed.

The Stoner exchange parameter estimated from magnetic measurements is within one order of magnitude of the electron-electron pairing coupling constant  $V 3k_B T_c = 1.0$  meV calculated in<sup>35</sup> for flat band superconductivity in graphite considering  $T_c = 4$  K. Despite using an expression obtained for multilayer graphene, we expect the order of magnitude of such estimation to be appropriate for bismuth as well, as the model developed in ref.<sup>35</sup> relies on a layered system with in-plane binding much stronger than interlayer coupling. Although less extreme than in graphite, such description is suited to bismuth<sup>3</sup>. The estimation of superconducting and ferromagnetic exchange interactions of about the same order of magnitude suggests a competition between both mechanisms, which can account both for conflicting reports on the properties of bismuth, as well as for the absence of superconductivity in our device.

Unfortunately, we are unable to tune the properties of our devices between ferromagnetism and superconductivity at will, as performed for multilayer graphene<sup>33</sup>. This happens because charge screening prevents the chemical potential in bulk Bi from being varied with a gate volt-

age. Instead, this modulation can be achieved through self-doping imposed by disorder or by adsorption of other elements at the sample surface/boundaries. As such, different samples are expected to show different properties, thus explaining diverging reports in the literature about the properties of Bi. Hence, we propose the interaction between a disordered surface (with grain boundaries and steps) and possibly adsorbed elements to be the responsible for the magnetism observed.

We close our discussion by mentioning that, while our report might seem surprising at first (the experiments are relatively straightforward and the magnetic fields involved are low), results hinting at the AHE in Bi have been previously reported by Conn and Donovan as early as 1948<sup>36,37</sup>. In their results, an anomalous negative MR below 40 mT was identified in Bi and attributed to a contribution due to the Hall effect. There, however, no hysteresis of the MR was attempted thus not allowing the attribution of the anomalous MR to ferromagnetism.

#### IV. CONCLUSION

In conclusion, in this work, we demonstrated the occurrence of the AHE in bismuth crystals. The phenomenon appears to be confined to the sample surface or grain boundaries, possibly being triggered by disorder at the interfaces. Circumstantial evidence such as similar tran-

sition temperatures, similar exchange energy parameters and behavior in the presence of magnetic fields - points towards a competition between magnetism and superconductivity, which can be understood in the context of the reconstruction of the Fermi surface of Bi along grain boundaries in a flat dispersion. The similarities between multilayer graphite and bismuth reported here are complementary to previous literature and suggest an universal origin for superconductivity in semimetals with low density of states near the Fermi level. We expect additional experiments in different systems to corroborate our hypothesis.

#### ACKNOWLEDGMENTS

We would like to thank Marta Cieplak for fruitful discussions. This work was supported by the National Science Center, Poland, research project no. 2016/23/P/ST3/03514 within the POLONEZ programme. The POLONEZ programme has received funding from the European Union's Horizon 2020 research and innovation programme under the Marie Skłodowska-Curie grant agreement No. 665778. P.G. acknowledges the support of the National Science Center, Poland, research project no. 2014/15/B/ST3/03889. Y. K. and A.A. were supported by CNPq and FAPESP.

\* camargo@ifpan.edu.pl

<sup>1</sup> L. Shubnikov and W. de Haas, Proceedings of the Academy of Sciences of Amsterdam **33**, 130 (1930).

<sup>2</sup> W. J. D. HAAS and P. M. V. ALPHEN., Proceedings of the Academy of Sciences of Amsterdam **33**, 1106 (1930).

<sup>3</sup> A. v. Ettingshausen and W. Nernst, Annalen der Physik **265**, 343 (1886), <https://onlinelibrary.wiley.com/doi/pdf/10.1002/andp.188626510>.

<sup>4</sup> O. Prakash, A. Kumar, A. Thamizhavel, and S. Ramakrishnan, Science **355**, 52 (2017), <http://science.sciencemag.org/content/355/6320/52.full.pdf>.

<sup>5</sup> F. Schindler, Z. Wang, M. G. Vergniory, A. M. Cook, A. Murani, S. Sengupta, A. Y. Kasumov, R. Deblock, S. Jeon, I. Drozdov, H. Bouchiat, S. Guron, A. Yazdani, B. A. Bernevig, and T. Neupert, Nature Physics **14**, 918 (2018).

<sup>6</sup> I. F. I. Mikhail and O. P. Hansen, Journal of Physics C: Solid State Physics **14**, L27 (1981).

<sup>7</sup> V. Edel'man, Advances in Physics **25**, 555 (1976), <https://doi.org/10.1080/00018737600101452>.

<sup>8</sup> "Bismuth (bi) effective masses: Datasheet from Landolt-Börnstein - group iii condensed matter · volume 41c: "non-tetrahedrally bonded elements and binary compounds i" in springermaterials ([https://doi.org/10.1007/10681727\\_1175](https://doi.org/10.1007/10681727_1175))," (), copyright 1998 Springer-Verlag Berlin Heidelberg.

<sup>9</sup> "Bismuth (bi) band structure, general: Datasheet from Landolt-Börnstein - group iii condensed matter · volume 41c: "non-tetrahedrally bonded ele-

ments and binary compounds i" in springermaterials ([https://doi.org/10.1007/10681727\\_1168](https://doi.org/10.1007/10681727_1168))," (), copyright 1998 Springer-Verlag Berlin Heidelberg.

<sup>10</sup> C. Orovets, A. Chamoire, H. Jin, B. Wiendlocha, and H. Heremans, Journal of Electronic Materials **41**, 1648 (2012).

<sup>11</sup> Y. Kopelevich, J. C. M. Pantoja, R. R. da Silva, and H. Moehlecke, Phys. Rev. B **73**, 165128 (2006).

<sup>12</sup> S. Koley, M. Laad, and A. Taraphder, Scientific Reports **7**, 10993 (2017).

<sup>13</sup> N. P. Armitage, R. Tediosi, F. Lévy, E. Giannini, L. Forro, and D. van der Marel, Phys. Rev. Lett. **104**, 237401 (2010).

<sup>14</sup> X. Du, S.-W. Tsai, D. L. Maslov, and A. F. Hebard, Phys. Rev. Lett. **94**, 166601 (2005).

<sup>15</sup> K. Behnia, M.-A. Méasson, and Y. Kopelevich, Phys. Rev. Lett. **98**, 166602 (2007).

<sup>16</sup> P. Kapitza and E. Rutherford, Proc. R. Soc. Lond. A **119**, 358 (1928).

<sup>17</sup> M. Sawicki, W. Stefanowicz, and A. Ney, Semicon. Sci. Technol. **26**, 064006 (2011).

<sup>18</sup> F. Muntyanu, Y. Dubkovetskii, and A. Gilevski, Phys. Solid State **46**, 18221824 (2004).

<sup>19</sup> D. Kechrakos and K. N. Trohidou, Phys. Rev. B **58**, 12169 (1998).

<sup>20</sup> X. Batlle, M. García del Muro, J. Tejada, H. Pfeiffer, P. Grnert, and E. Sinn, Journal of Applied Physics **74**, 3333 (1993), <https://doi.org/10.1063/1.354558>.

<sup>21</sup> K. Gas and M. Sawicki, Measurement Science and Technology **30**, 085003 (2019).

<sup>22</sup> J. Crangle and G. M. Goodman, Proceedings of the Royal Society of London. Series A, Mathematical and Physical Sciences **321**, 477 (1971).

<sup>23</sup> P. Hu, L. Kang, T. Chang, F. Yang, H. Wang, Y. Zhang, J. Yang, K. she Wang, J. Du, and Z. Yang, Journal of Alloys and Compounds **728**, 88 (2017).

<sup>24</sup> K. Ho, X. Xiong, J. Zhi, and L. Cheng, Journal of Applied Physics **74**, 6788 (1993), <https://doi.org/10.1063/1.355078>.

<sup>25</sup> T. Hirahara, I. Matsuda, S. Yamazaki, N. Miyata, S. Hasegawa, and T. Nagao, Applied Physics Letters **91**, 202106 (2007), <https://doi.org/10.1063/1.2813613>.

<sup>26</sup> B. Weitzel and H. Micklitz, Phys. Rev. Lett. **66**, 385 (1991).

<sup>27</sup> D. Gitsu, A. Grozav, G. Kistol, N. Leporda, and F. Muntyanu, JETP Letters **55**, 403 (1992).

<sup>28</sup> D. W. Boukhvalov, S. Moehlecke, R. R. da Silva, and Y. Kopelevich, Phys. Rev. B **83**, 233408 (2011).

<sup>29</sup> F. M. Muntyanu, A. Gilewski, K. Nenkov, J. Warchulska, and A. J. Zaleski, Phys. Rev. B **73**, 132507 (2006).

<sup>30</sup> T. Hamada, K. Yamakawa, and F. E. Fujita, Journal of Physics F: Metal Physics **11**, 657 (1981).

<sup>31</sup> D. Kim, *New perspectives in Magnetism of Metals, Ch.3* (Springer US, 1999).

<sup>32</sup> D. Papaconstantopoulos, *Handbook of the Band Structure of Elemental Solids* (Springer US, 2015).

<sup>33</sup> V. J. Kauppila, F. Aikebaier, and T. T. Heikkilä, Phys. Rev. B **93**, 214505 (2016).

<sup>34</sup> X. Liu, Z. Hao, E. Khalaf, J. Lee, K. Watanabe, T. Taniguchi, A. Vishwanath, and P. Kim, arXiv: 1903.08130 (2019).

<sup>35</sup> N. B. Kopnin, T. T. Heikkilä, and G. E. Volovik, Phys. Rev. B **83**, 220503(R) (2011).

<sup>36</sup> B. Donovan and G. Conn, The London, Edinburgh, and Dublin Philosophical Magazine and Journal of Science **41**, 770 (1950), <https://doi.org/10.1080/14786445008561009>.

<sup>37</sup> G. Conn and B. Donovan, Nature **162**, 336 (1948).